Identification of Sequences Responsible for Intracellular Targeting and Membrane Binding of Rat CYP2E1 in Yeast†

Etienne P. A. Neve,‡,§ Mats Hidestrand‡, and Magnus Ingelman-Sundberg*

Division of Molecular Toxicology, Institute of Environmental Medicine, Karolinska Institutet, SE-171 77 Stockholm, Sweden

Received July 14, 2003; Revised Manuscript Received September 30, 2003

ABSTRACT: The role of the hydrophobic NH_2-terminal domain of rat CYP2E1 for intracellular targeting and membrane binding was investigated in *Saccharomyces cerevisiae* as a model system. Several different CYP2E1 variants with deletions and mutations were expressed in yeast, and their intracellular localization and membrane-binding properties were analyzed. We found that an amino acid stretch including the B-helix from glycine 82 to aspargine 95 is responsible for mitochondrial association of CYP2E1 in yeast. Furthermore, we investigated the membrane-binding properties of the variants and concluded that the same region in the B-helix is responsible for membrane interactions of CYP2E1 by electrostatic interactions. A soluble variant of CYP2E1 lacking the first 82 amino acids and containing leucine to aspartate amino acid exchanges at positions 90 and 91, which disrupted the amphipathic nature of the B-helix, was expressed at relatively high levels in the yeast and was found to be catalytically active toward chlorzoxazone in cumene hydroperoxide-supported reactions. We suggest that these amino acid changes at positions 90 and 91 abolish the electrostatic interaction between the negatively charged membrane and the positively charged B-helix, thereby producing a soluble product.

In eukaryotes, xenobiotic-metabolizing cytochrome P450s (P450s)[1] are localized in the membrane of the endoplasmic reticulum (ER), where they are cotranslationally inserted in a signal recognition particle- (SRP-) dependent manner (*1*−*3*). The hydrophobic NH_2-terminal domain of P450 plays an important role not only in the targeting to and insertion into the ER membrane but also in the anchoring and retention of the protein in the ER (*4*−*6*).

Cytochrome P450 2E1 (CYP2E1), the alcohol-inducible member of the P450 family, has been shown to be involved in gluconeogenesis, especially under fasting conditions, and has a central role in metabolism of fatty acids (*7*, *8*). CYP2E1 is well-known for its ability to convert various xenobiotics into carcinogenic or toxic metabolites (*8*), and knockout experiments in mice have revealed its importance in benzene, acrylonitrile, azoxymethane, and acetaminophen toxicity (*9*−*11*). In addition, CYP2E1 produces reactive oxygen species that can initiate lipid peroxidation (*12*), resulting in apoptosis in hepatoma cells (*13*), or can cause activation of hepatic Stellate cells, resulting in collagen expression with potential risk for the development of fibrosis (*14*).

CYP2E1 is mainly present in the ER membrane, although significant expression has also been detected in lysosomes (*15*), Golgi apparatus (*16*), peroxisomes (*17*), and the plasma membrane (*18*, *19*). The majority of CYP2E1 was demonstrated to be retained in the ER membrane through a retrieval mechanism, and inhibition of the retrograde transport results in accumulation of CYP2E1 in the Golgi apparatus (*6*). The transport to the plasma membrane is explained by an erroneous insertion of a small fraction of CYP2E1 in the ER with a lumenal orientation and subsequent transport via the Golgi apparatus to the plasma membrane (*19*).

Experiments in hepatoma cells revealed that transiently expressed CYP2E1 cDNA variants lacking the hydrophobic NH_2-terminal transmembrane domain or containing mutations in this region caused the formation of an enzyme specifically targeted to mitochondria. After import into mitochondria, these CYP2E1 variants were further NH_2-terminally truncated to produce a mature mitochondrial form of the protein, Δ2E1 lacking about 100 amino acids. This form of CYP2E1 was shown to be a soluble catalytically active protein and was also found to be present in small amounts in isolated rat liver mitochondria (*20*, *21*). These findings implied that the membrane-spanning parts are located in the most NH_2-terminal moiety of the protein while at the same time demonstrating that the remainder of the protein does not contain any additional stop-transfer signals.

† This study was supported by grants from the Swedish Research Council.

* Address correspondence to this author at the Division of Molecular Toxicology, IMM, Karolinska Institutet, Box 210, SE-171 77 Stockholm, Sweden. Tel +468-5248-7735; fax +468-337-327; e-mail magnus.ingelman-sundberg@imm.ki.se.

‡ Both authors contributed equally.

§ Present address: Ludwig Institute for Cancer Research, Stockholm Branch, Karolinska Institutet, Sweden.

[1] Abbreviations: P450, cytochrome P450; SRP, signal recognition particle; ER, endoplasmic reticulum; prot K, proteinase K; NaDOC, sodium deoxycholate; wt, wild-type; Δ29-2E1, Δ64-2E1, Δ82-2E1, and Δ95-2E1, CYP2E1 variants with a NH_2-terminal methionine but lacking 29, 64, 82, and 95 amino acids from the NH_2-terminal region, respectively; Δ82mut-2E1, as Δ82-2E1 but with the amino acid exchanges leucine to aspartate at positions 90 and 91; Dpm1p, dolichol phosphate mannose synthase; DMSO, dimethyl sulfoxide; EDTA, ethylenediaminetetraacetic acid; Hepes, *N*-(2-hydroxyethyl)piperazine-*N*′-2-ethanesulfonic acid; MOPS, 3-(*N*-morpholino)propanesulfonic acid; NADPH, reduced nicotinamide adenine dinucleotide phosphate; Tris, tris(hydroxymethyl)aminomethane.

10.1021/bi035193s CCC: $25.00
Published on Web 11/15/2003

Table 1: Sequences of the Oligonucleotides Used as Polymerase Chain Reaction Primers[a]

primer	sequence (5′ to 3′)
wtF (1−18)	GAC*TGATCA*ATGGCGGTTCTTGGCATC
Δ29F (88−105)	GAC*TGATCA*ATGTGGAACCTGCCCCCAGGA
Δ64F (193−213)	GAC*TGATCA*ATGGGGCCAGTGTTCACACTGCAC
Δ82F (247−267)	GAC*TGATCA*ATGTACAAGGCTGTCAAGGAGGTG
Δ95F (286−306)	GAC*TGATCA*ATGGAGTTTTCTGGACGGGGGGAC
N^{2+}F (1−27)	GAC*TGATCA*ATGAAGAGGCTTGGCATCACCATTGCC
wtR (1465−1482)	GAC*GAATTC*TCATGAACGGGGAATGAC
Δ82mutF (244−294)	GGCTACAAGGCTGTCAAGGAGGTGGACGACAACCACAAGAATGAGTTTTCT
Δ82mutR (246−296)	CCAGAAAACTCATTCTTGTGGTTGTCGTCCACCTCCTTGACAGCCTTGTAG

[a] The bases that were mutated are underlined, and restriction sites are depicted in italic type. The positions of the bases in the wtCYP2E1 sequence are indicated in parentheses.

Saccharomyces cerevisiae or bakers' yeast has proven to be a useful model system for the expression of mammalian proteins (*22*, *23*). Being a eukaryote, yeast has a similar cellular organization and similar mechanisms in protein translocation, secretion, and posttranslational modification as mammalian cells. Yeast has been successfully utilized for heterologous expression of different forms of P450 that were used for metabolic studies (*24*−*26*). When expressed in yeast, CYP2D6 was detected at the plasma membrane (*27*), which indicated that yeast could also be used as a model system to study the intracellular transport and targeting of mammalian P450s. Many components of the mitochondrial protein import machinery, such as cytosolic factors and the receptors present both in the mitochondrial outer and inner membrane, are well conserved between mammalian and yeast cells (*28*, *29*). Components isolated from yeast mitochondria have successfully been used to study the mitochondrial targeting of the precursor to bovine adrenal adrenodoxin (*30*).

In the present study we have investigated the role of the hydrophobic NH_2-terminal transmembrane domain of rat CYP2E1 for intracellular targeting and membrane association when expressed in yeast. Although similarities in intracellular targeting of these NH_2-terminally truncated and modified forms of CYP2E1 were shown to exist between the yeast and the mammalian cells, differences were observed in mitochondrial import and processing. In addition, we were able to map that the region between amino acids 64 and 95 was responsible for mitochondrial association and that a motif between amino acids 82 and 94, the so-called B-helix, was responsible for membrane interactions. By mutagenesis of two hydrophobic amino acids to negatively charged residues in this region, a soluble and catalytically active form of the protein was engineered.

EXPERIMENTAL PROCEDURES

Yeast Strain and Growth Conditions. The yeast strain W(R) was used, which has been engineered from W303-1B (*MAT a leu2-3112 his3-11 ade2-1 trp1-1 ura3-1 can*^{R} *cyr*$^+$) to overexpress the yeast NADPH cytochrome P450 reductase utilizing a galactose-inducible promoter (*26*). This strain was transformed by use of lithium acetate with the pYeDP60 plasmid, which contains the galactose promoter and the URA3 and ADE2 selection markers (*26*). Transformants were selected and grown in synthetic galactose/tryptophan (SLI) medium at 28 °C by a low-density protocol until an OD_{600} of 0.8−1.5 was reached as described (*26*). This method is more cautious to the cell organelle organization, but to achieve P450 levels that could be spectrally determined, a high-density expression protocol was used. In this protocol the yeast is grown at 28 °C to an OD of 10 in energy-rich medium with glucose as energy source. When the culture reached the correct optical density, the temperature was lowered to room temperature and the expression was started by addition of galactose. Apart from the temperature change, this procedure is described in ref *24*.

Plasmids. The expression vector used was pYeDP60 (V60), a galactose-inducible yeast expression vector carrying the 2μ origin of replication and the URA3 and ADE2 selection markers (*26*). The wild-type CYP2E1 (wt2E1) insert was generated by PCR amplification with *Pfu* DNA polymerase (Stratagene, La Jolla, CA), rat CYP2E1 cDNA as a template, and the wt forward primer and wt reverse primer (Table 1). NH_2-terminally truncated CYP2E1 constructs were generated by PCR amplification with forward primer for either Δ29-2E1, Δ64-2E1, Δ82-2E1, and Δ95-2E1 together with the wt reverse primer as shown in Table 1. N^{2+}2E1 containing A2K and V3R substitutions was created by PCR amplification with the N^{2+} forward primer that incorporated these mutations and wt reverse primer. All CYP2E1 constructs were inserted between the *Bam*HI and *Eco*RI sites of the V60 expression vector. Additional mutations in the truncated variants including Δ82-2E1 L90D and L91D (Δ82mut-2E1) were generated by use of the Qiagen site-directed mutagenesis kit according to the manufacturer's recommendation. The correct sequence of the inserts was confirmed by automated DNA sequencing with the ABI PRISM dye terminator cycle sequencing kit from Perkin-Elmer.

Western Blot Analysis and Antibodies. Proteins were separated by SDS−polycarylamide gel electrophoresis and transferred to nitrocellulose membranes that were blocked and incubated with the appropriate antibodies (*16*). Monoclonal antibodies directed against yeast proteins were purchased from Molecular Probes (Molecular Probes Europe, Leiden, The Netherlands). Endoplasmic reticulum was detected by dolichol phosphate mannose synthase (Dpm1p) antibodies. Mitochondria were detected by anti-mitochondrial porin antibodies and vacuoles by anti-vacuolar H^+-ATPase (V-ATPase) antibodies. In addition, antibodies recognizing the ER lumenal protein KAR2p were a generous gift from Per Ljungdahl (Ludwig Institute for Cancer Research, Stockholm, Sweden).

Subcellular Fractionation. Yeast cells were grown in SLI medium to an OD_{600} of 0.8−1.5 and harvested. The cell wall was enzymatically removed by use of yeast lytic enzyme (ICN Biochemicals) according to the manufacturer's instruc-

tions. The spheroplasts were lysed with 50 strokes of a tissue grinder (Kontes Scientific Glassware; pestle B) and the lysate was spun 10 min at 2000*g* to remove unbroken cells and debris. Two milliliters of the postnuclear supernatant was loaded on top of a discontinuous sucrose gradient consisting of 1 mL each of 12%, 18%, 24%, 30%, 36%, 42%, 48%, and 54% (w/v) sucrose and a 0.5 mL step of 60% (w/v) sucrose and centrifuged for 4 h 40 min at 100000*g* in a SW41 Ti rotor (Beckman Instruments) (*31, 20*). Fractions (1 mL) were collected from bottom to top after the bottom of the centrifuge tube was punctured, and aliquots were analyzed by Western blotting for the presence of organelle marker proteins and the CYP2E1 variants.

Membrane Association. Membrane association of the expressed CYP2E1 variants was assessed in sodium bicarbonate (Na_2CO_3) (*32*) and in different concentrations of potassium phosphate buffer. The postnuclear supernatant obtained from yeast expressing the different CYP2E1 variants was diluted either in 0.1 M Na_2CO_3, pH 11.5, to a protein concentration of 0.25 mg/mL or in 150 or 500 mM potassium phosphate, pH 7.4, to a protein concentration of 1 mg/mL and incubated for 30 min at 4 °C on a vertical rotating platform. The membranous (consisting of both mitochondrial and microsomal membranes) and soluble fractions were isolated by centrifugation for 60 min at 100000*g* at 4 °C. Both fractions were analyzed by Western blotting for the presence of the CYP2E1 variants and the marker proteins.

Membrane Topology. The membrane topology was determined by protease protection assay with proteinase K (prot K) and the subcellular fractions containing the different CYP2E1 variants, i.e., the microsomal fraction for wt2E1, N^{2+}2E1, and Δ95-2E1 and the mitochondrial fraction for Δ29-2E1 and Δ64-2E1. The fractions were diluted with 50 mM Tris-HCl buffer, pH 8.0, containing 150 mM NaCl and 10 mM $CaCl_2$ to a protein concentration of 1 mg/mL and incubated with or without prot K (25 or 50 μg/mL) in the presence or absence of 0.5% Triton for 25 min at 37 °C. The digestion was stopped by the addition of an equal volume of ice-cold 50% trichloroacetic acid. Proteins were allowed to precipitate on ice for 30 min and were subsequently centrifuged, dissolved in SDS−PAGE sample buffer, and analyzed by Western blotting.

Digitonin fractionation was carried out essentially as described in Hartl et al. (*33*). In brief, yeast cells were grown according to the low-density protocol and mitochondria were prepared by differential centrifugation. The mitochondria were washed four times by resuspending the 9500*g* pellet in 7 mL of mitochondrial buffer (0.6 M mannitol, 20 mM Hepes, pH 7.4, 0.6 M sucrose, 3 mM $MgCl_2$, and 3 mM ATP). The mitochondrial pellet was finally resuspended in 50 μL of mitochondrial buffer and total protein content was determined. The digitonin fractionation was carried out with digitonin (stock solution of 8% in DMSO) at concentrations ranging from 0.04% to 0.4% at 4 °C. Digitonin and SEOMK buffer (250 mM sucrose, 5 mM EDTA, 10 mM MOPS, pH 7.2, 200 mM KCl, and 0.5 mM phenanthroline) were placed at the bottom of an eppendorf and 50 μg of mitochondria was placed at the side of the tube. One-minute reactions were started by a brief vortex and stopped by diluting the sample 5 times with SEOMK buffer and centrifuging for 1 h at 100000*g*. The pellet was dissolved in a volume corresponding to that of the supernatant, and similar amounts of pellet and supernatant were analyzed by Western blot.

Catalytic Activity. The catalytic activity of the CYP2E1 variants was determined by monitoring the formation of 6-hydroxychlorzoxazone from chlorzoxazone (*16*). The incubation mixtures contained 100 μg of microsomal or mitochondrial protein, an NADPH-generating system (0.2 mM NADPH, 2.0 mM glucose 6-phosphate, and 3 units/mL glucose-6-phosphate dehydrogenase), and 50 μM chlorzoxazone in 100 mM phosphate buffer, pH 7.4. After 30 min of incubation at 37 °C, the reaction was terminated by the addition of orthophosphoric acid, followed by the addition of an internal standard (acetaminophen), and incubation mixtures were extracted with dichloromethane. The same procedures were applied when cumene hydroperoxide was used as an electron donor instead of the NADPH-generating system. In such incubations 400 μg of protein were used, the NADPH was exchanged for 100 μM cumene hydroperoxide, the chlorzoxazone concentration was 500 μM, and the incubation time was 2.5 or 30 min. All samples were analyzed on a Varian ProStar HPLC system (Varian, Walnut Creek, CA) equipped with an amperometric detector (Bioanalytical Systems Inc, West Lafayette, IN).

Homology Model. Homology modeling of rat CYP2E1 was done by using the SWISS-MODEL facility at http://expasy.ch/swissmod/. Template coordinates used were those of CYP2C5 (*34*). Graphical representation was made by use of ICM lite version 2.8 (Molsoft LLC, La Jolla, CA).

RESULTS

Yeast cells were transformed with the V60 plasmid containing the cDNA inserts for the different CYP2E1 constructs (Figure 1A), selected and grown according to the low-density protocol (*26*). The constructs used, besides the wt protein, were N^{2+}2E1, which contains two additional positive charges at the very NH_2-terminus resulting in a more lumenal orientation of the protein in hepatoma cells (*19*); Δ29-2E1, without the distal NH_2-terminal membrane spanning region; Δ64-2E1, without the most NH_2-terminally oriented putative mitochondrial targeting signal; Δ82-2E1, where half of the second putative mitochondrial targeting sequence has been removed; Δ82mut-2E1, where the two leucines at positions 90 and 91 have been replaced by the negatively charged amino acid aspartate; and Δ95-2E1, where both putative mitochondrial targeting signals have been removed. Cells were harvested, and after enzymatic removal of the cell wall, the spheroplasts were homogenized and the postnuclear supernatant was analyzed by Western blot analysis (Figure 2). Yeast transformed with wt2E1 produced a protein with an apparent molecular weight of about 52 kDa, corresponding to rat CYP2E1, while in yeast transformed with the empty plasmid (V60) no CYP2E1 protein could be detected. A protein with similar mobility as wt2E1 was observed in cells transformed with the N^{2+}-2E1 construct. Yeast transformed with the NH_2-terminally truncated CYP2E1 forms Δ29-2E1, Δ64-2E1, Δ82-2E1, Δ82mut-2E1, and Δ95-2E1 produced proteins that all displayed a mobility corresponding to their predicted full-length and all variants were expressed at similar levels. Thus, in contrast to the situation in hepatoma cells (*19*), no bands of higher mobility were detectable, indicating that no processing of these proteins occurred in yeast.

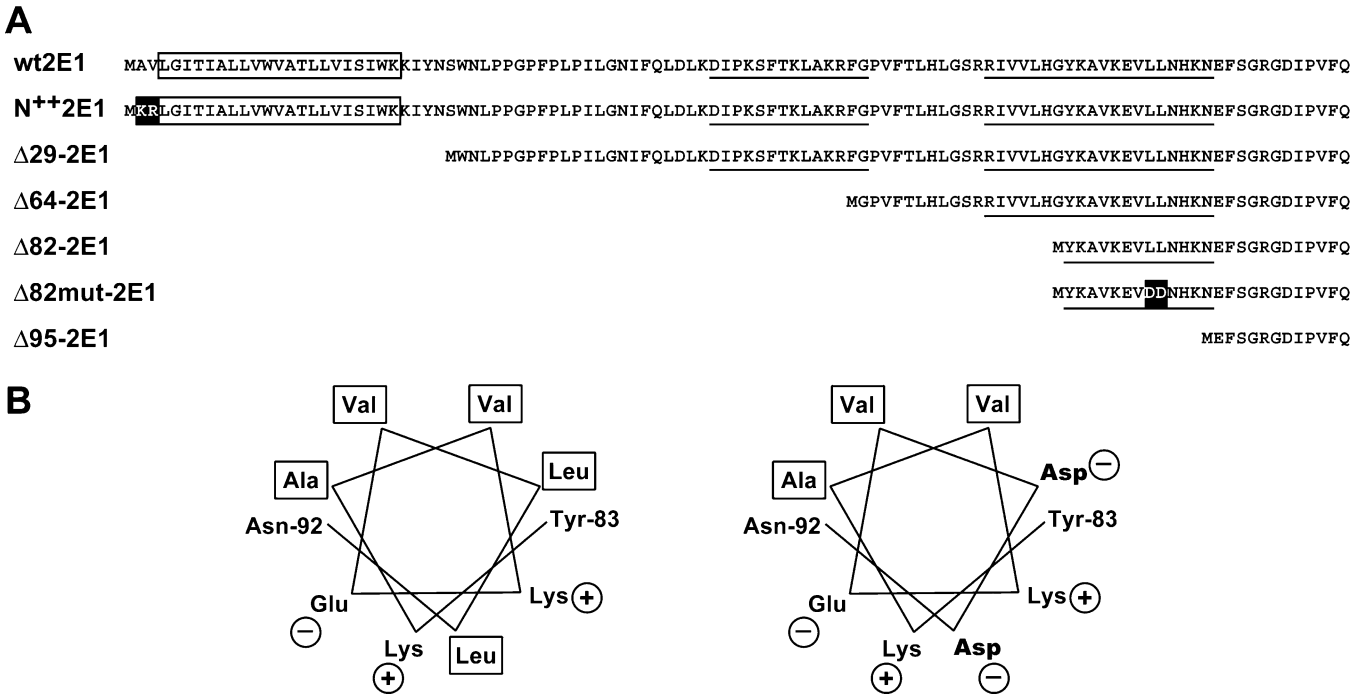

FIGURE 1: (A) Schematic representation of the NH_2-terminally truncated CYP2E1 constructs used in this study. Only the NH_2-terminal regions of CYP2E1 and its truncated variants are shown. The hydrophobic transmembrane domain is represented in a box, the putative mitochondrial targeting sequences are underlined, and the amino acid residues that are mutated in N^{2+}2E1 and Δ82mut-2E1 are shown against a black background. (B) Helical wheel plot of the region of CYP2E1 between amino acids 83 and 92. The helical wheel for wt2E1 is shown on the left side, and the wheel where leucines at positions 90 and 91 were substituted with aspartates (residues indicated in boldface type) is shown on the right. Hydrophobic residues are shown in boxes and residues carrying a charge are indicated by + or −.

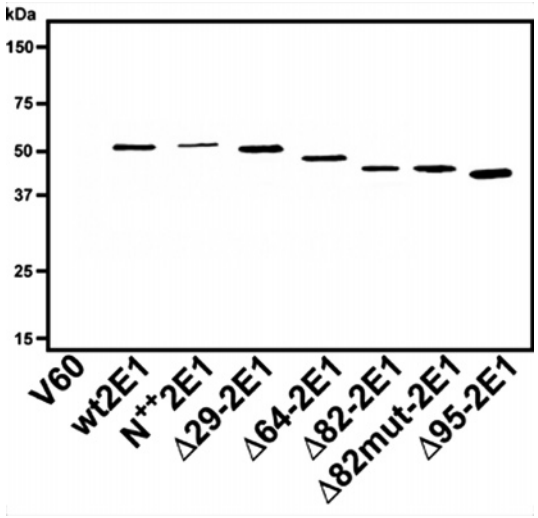

FIGURE 2: Expression of wt2E1, N^{2+}2E1, Δ29-2E1, Δ64-2E1, Δ82-2E1, Δ82mut-2E1, and Δ95-2E1 proteins. The postnuclear supernatants isolated from the yeast strains transformed with these CYP2E1 constructs as well as the empty vector V60 were separated by SDS−PAGE and analyzed by Western blotting with CYP2E1-specific antibodies.

The postnuclear supernatant from the transformed yeast was fractionated by centrifugation into a 10000*g* pellet (mitochondrial fraction), 100000*g* pellet (microsomal fraction), and 100000*g* supernatant (cytosolic fraction) and analyzed by Western blotting (Figure 3). The highest levels of wt2E1 and N^{2+}2E1 were observed in the 100000*g* pellet with no protein visible in the cytosolic fraction, indicating that these proteins are membrane-bound. The highest levels of Δ29-2E1, Δ64-2E1, and to a lesser extent Δ82-2E1 were found in the 10000*g* pellet, indicating that they were associated with the mitochondria. The Δ82-2E1 was more prone to proteolytic degradation than the other variants if the OD_{600} of the cultures increased over 1.0 as illustrated in Figure 3 by the appearance of a band with higher mobility. The majority of Δ82mut-2E1 and Δ95-2E1 was recovered in the microsomal fraction, although a significant amount of these proteins was also found in the 100000*g* supernatant, suggesting that they are loosely associated with the membranes of this fraction.

To more accurately determine the intracellular distribution of the CYP2E1 variants, the postnuclear supernatants were fractionated on discontinuous sucrose gradients (Figure 4). As shown at the bottom of the figure, the mitochondrial, microsomal, and vacuolar fractions were well separated from each other. Wt2E1 and N^{2+}2E1 were recovered in fraction numbers 4, 5, and 6 and cofractionated nicely with the ER marker Dpm1p. Δ29-2E1 was exclusively found in the mitochondrial fraction, while for Δ64-2E1, although the majority of the protein was recovered in the mitochondrial fraction, a significant amount was also found to be associated with the vacuolar fraction. Δ82-2E1, however, displayed a more broad distribution, with the highest amounts found in mitochondrial and vacuolar fractions with minor amounts in the ER fractions. In contrast to Δ82-2E1, Δ82mut-2E1 as well as Δ95-2E1 was solely recovered in the vacuolar fractions.

The membrane association of the CYP2E1 variants was determined by sodium bicarbonate treatment and treatment with a high concentration of potassium phosphate for the examination of mainly ionic interactions (Figure 5). When the postnuclear supernatant of yeast expressing the various constructs was treated with 0.1 M Na_2CO_3, integral membrane proteins such as the ER protein Dpm1p and the

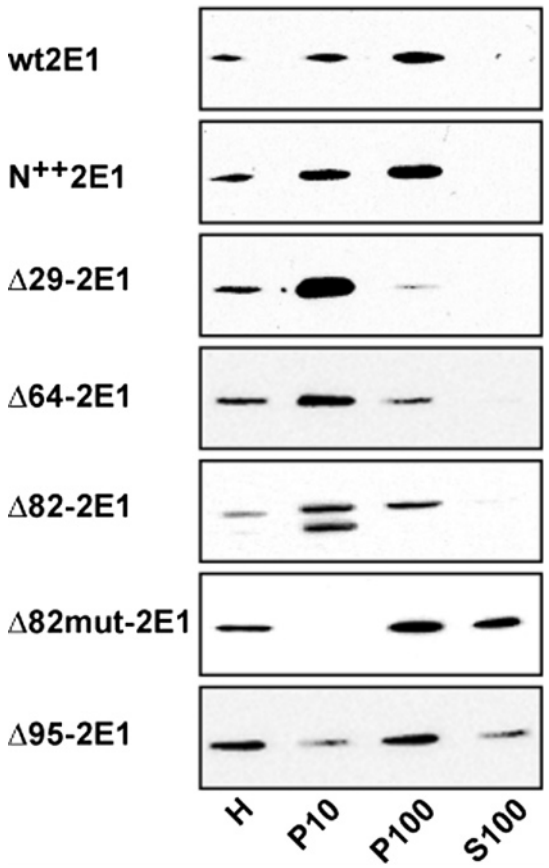

FIGURE 3: Subcellular distribution of wt2E1, N^{2+}2E1, Δ29-2E1, Δ64-2E1, Δ82-2E1, Δ82mut-2E1, and Δ95-2E1 as revealed by differential centrifugation. Yeast strains expressing the different CYP2E1 variants were grown to an OD_{600} of 0.8−1.5 and fractionated by centrifugation into a 10000*g* pellet (P10), 100000*g* pellet (P100), and the cytosol (S100). Similar amounts of homogenate (H), P10, P100, and S100 were analyzed by Western blot analysis.

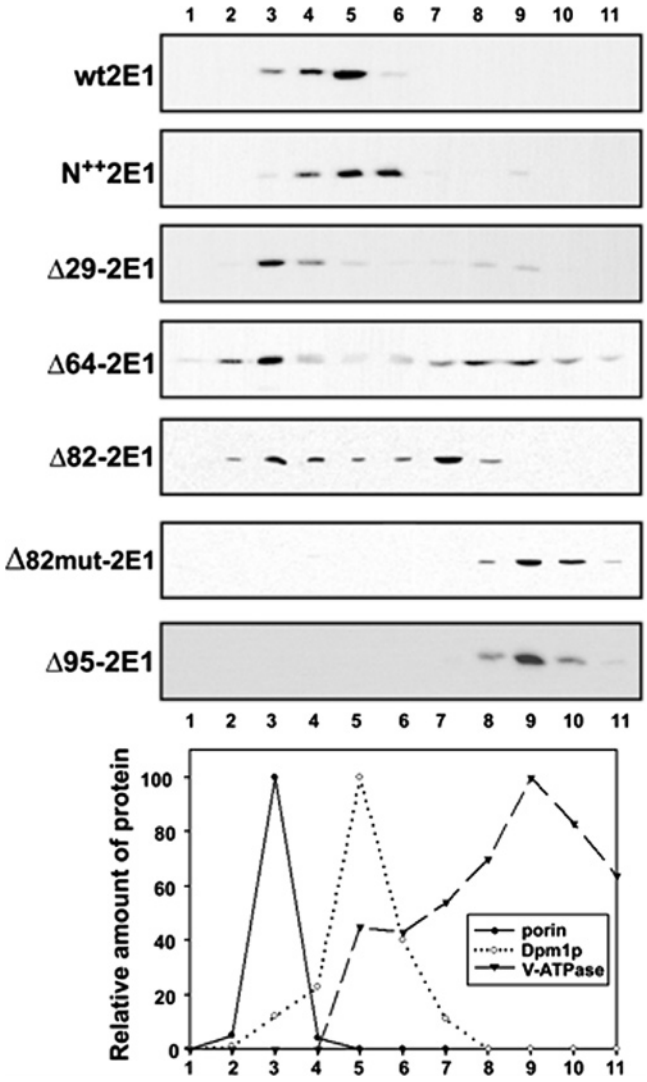

FIGURE 4: Intracellular localization of the CYP2E1 variants determined by discontinuous sucrose density gradients. Yeast strains expressing the various CYP2E1 constructs were grown to an OD_{600} of 0.8 according to the low-density protocol and homogenized after enzymatic removal of the cell wall. The postnuclear supernatant was layered on top of a discontinuous sucrose gradient and centrifuged. Fractions (1 mL) were collected from bottom to top by puncturing the bottom of the centrifuge tube. Aliquots of each fraction were analyzed by Western blotting with CYP2E1-specific antibodies, Dpm1p-specific antibodies (an ER marker), porin-specific antibodies (a mitochondrial marker), and V-ATPase-specific antibodies (as a marker for the vacuoles). In the graph at the bottom of the figure, a typical distribution of these marker proteins in these gradients is shown.

mitochondrial protein porin remained associated with the membranous fraction, whereas the majority of the peripheral and soluble proteins, such as the soluble lumenal ER protein KAR2p, were recovered in the soluble fraction (Figure 5A, bottom panel). Wt2E1 and N^{2+}2E1 were exclusively recovered in the membranous fraction, confirming that they are integral membrane proteins (Figure 5A, upper panel). Deletion of the NH_2-terminal hydrophobic transmembrane domain as in Δ29-2E1 did not have any significant effect on the membrane association and only a tiny fraction of Δ29-2E1 was found in the soluble fraction. This suggests that Δ29-2E1 is tightly associated with the mitochondrial membrane. A similar observation was made for Δ64-2E1: despite the extensive NH_2-terminal deletion, this protein still was strongly associated with the membranes of the mitochondria. Deletion of the first 82 amino acids as in Δ82-2E1 resulted in about equal amounts in the membranous and soluble fraction. A similar observation was made for Δ95-2E1, indicating that additional truncation did not affect the membrane association of these mutants. Only when, in addition to deletion of the first 82 amino acids, both leucines at positions 90 and 91 were exchanged with aspartates (Δ82mut-2E1) was a profound effect observed: almost all protein was found in the supernatant. The extent of membrane association of wt2E1, Δ64-2E1, Δ82-2E1, and Δ82mut-2E1 was also evaluated by treatment of the postnuclear supernatant with 150 or 500 mM potassium phosphate buffer (Figure 5B). As for the carbonate treatment, in 150 mM phosphate buffer the wt2E1 and Δ64-2E1 variants were only found in the pellet. Only a small fraction of Δ82-2E1, being expressed at significantly lower levels, was present in the supernatant after treatment with 150 mM phosphate. In contrast, Δ82mut-2E1 was almost completely recovered in the supernatant; only a small fraction was found in the pellet. Increasing the ionic strength of the buffer to 500 mM phosphate did not alter the distribution of the wt2E1 while only some minor solubilization was observed for Δ64-2E1, confirming their strong association with the mitochondrial membrane. Treatment of Δ82-2E1 with 500 mM phosphate, however, resulted in almost complete release of the protein

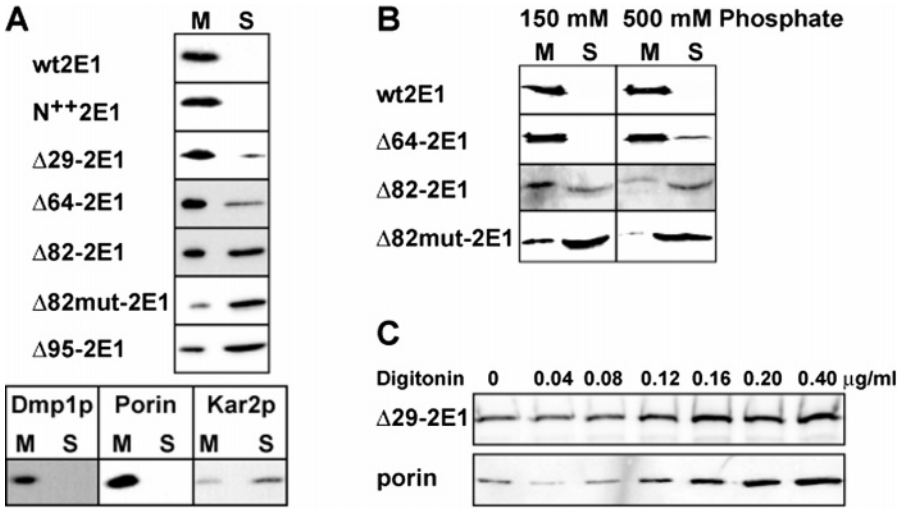

FIGURE 5: Membrane association of the CYP2E1 variants. (A) Sodium bicarbonate (Na_2CO_3) treatment. The postnuclear supernatants of yeast cells expressing the CYP2E1 variants were treated with 0.1 M Na_2CO_3, and the membranous (M) and soluble (S) fractions were separated by ultracentrifugation and analyzed by Western blotting for the presence of CYP2E1, Dpm1p (an ER integral membrane protein), porin (an integral membrane protein located in the mitochondrial outer membrane), and KAR2p (a soluble lumenal ER protein). The marker protein blots are shown at the bottom of the panel. (B) Potassium phosphate treatment. The postnuclear supernatants of yeast cells expressing the wt2E1, Δ64-2E1, Δ82-2E1, and Δ82mut-2E1 variants were treated with 150 or 500 mM potassium phosphate, pH 7.4. The membranous (M) and soluble (S) fractions were separated by ultracentrifugation and analyzed by Western blotting with antibodies specific for CYP2E1. (C) Digitonin fractionation of mitochondria isolated from yeast expressing Δ29-2E1. Mitochondria were incubated with an increasing concentration of digitonin, after which the solubilized proteins were isolated by ultracentrifugation and analyzed by Western blot for the presence of Δ29-2E1 and porin as a marker for the efficiency of removal of the mitochondrial outer membrane.

in the supernatant. Similar treatment of Δ82mut-2E1 did not result in dramatic changes. These results indicate that the major forces for membrane interaction of the Δ82-2E1 as well as the Δ82mut-2E1 variant are ionic in nature.

The membrane topology of the CYP2E1 variants was determined by protease protection assay with proteinase K (prot K) in the absence or presence of the detergent Triton X-100 (Figure 6). Wt2E1, N^{2+}2E1, Δ64-2E1, and Δ95-2E1 were all completely digested with the lowest concentration of prot K (25 μg/mL), conditions that also digested the cytoplasmic-oriented Dpm1p. However, the ER-lumenal marker KAR2p was unaffected by the same amount of prot K. This indicates that all these CYP2E1 variants have a cytoplasmic orientation in their respective membranes being ER, mitochondria, or vacuoles. Δ29-2E1 appeared slightly more resistant toward digestion, and complete digestion was only observed at the highest concentration of prot K (50 μg/mL), under conditions at which the lumenal marker protein KAR2p was also somewhat affected.

To establish the precise localization of Δ29-2E1, mitochondria were isolated and treated with increasing amounts of digitonin to selectively remove the mitochondrial outer membrane. As illustrated in Figure 5C, lower panel, increasing amounts of digitonin release porin, an integral component of the mitochondrial outer membrane, into the supernatant. Similarly, Δ29-2E1 was released in the same fractions, indicating that Δ29-2E1 is associated with the mitochondrial outer membrane.

The catalytic activities of the CYP2E1 variants were determined by monitoring the hydroxylation of the CYP2E1 substrate chlorzoxazone in the presence of NADPH or cumene hydroperoxide as an alternative electron donor. As summarized in Table 2, all CYP2E1 variants except Δ82mut-2E1 and Δ95-2E1 displayed catalytic activity toward chlorzoxazone when NADPH was used as an electron donor. This might indicate that the more soluble forms (Δ82mut-2E1 and Δ95-2E1) of the enzyme have lost their ability to interact with the membrane-bound NADPH−cytochrome P450 reductase, which is present in these yeast strains (*26*). Reconstitution of Δ95-2E1 expressed in yeast with the mammalian mitochondrial electron carriers adrenodoxin and adrenodoxin reductase also did not result in any significant catalytic activity toward chlorzoxazone (data not shown). Similarly, reconstitution of Δ29-2E1, Δ64-2E1, and Δ82-2E1 with these mitochondrial electron carriers did not result in any enhancement in the catalytic activity. These results indicate that these enzyme variants were not able to efficiently couple with these soluble mitochondrial electron-transfer proteins. Additionally, the catalytic properties of the variants were analyzed with cumene hydroperoxide (100 μM) as electron donor. Wt2E1, Δ82mut-2E1, and Δ95-2E1 (Table 2) all displayed significant catalytic activity toward chlorzoxazone when incubated in the presence of cumene hydroperoxide, although the truncated forms displayed lower activity levels as compared to the wt form. Because of its interesting properties being both soluble and catalytically active, the Δ82mut-2E1 variant was studied in more detail. The Δ82mut-2E1 variant was expressed in yeast by the high-density culture protocol in order to obtain higher amounts (see Experimental Procedures). It was found that the expression was temperature-dependent and optimal conditions were obtained at room temperature instead of the usually used 28 °C. The enzyme in its soluble form exhibited an absorption spectrum in the reduced CO-bound form, indicating a correct fold (Figure 7A). The specific catalytic activity supported by cumene hydroperoxide was determined to be around 4.77 pmol of 6-OH chlorzoxazone (pmol of P450)$^{-1}$ min^{-1} when the background activity was subtracted (Figure 7B). Finally the specific catalytic activity for Δ82mut-2E1 was found to be about 35% that found for wt2E1. Thus, these results show the successful engineering of CYP2E1 to a soluble, correctly folded, catalytically active enzyme.

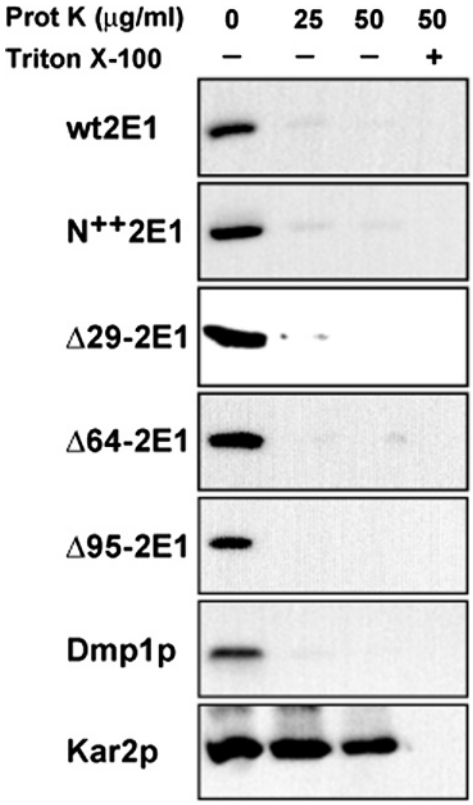

FIGURE 6: Membrane topology of the CYP2E1 variants as determined by a protease protection assay. The mitochondrial (containing Δ29-2E1 and Δ64-2E1) or the microsomal (containing wt2E1, N^{2+}2E1, and Δ95-2E1) fractions were incubated with or without proteinase K (prot K) in the presence or absence of Triton X-100 (0.5%) as indicated. The reaction was terminated by the addition of trichloroacetic acid, and the precipitated proteins were dissolved in SDS−PAGE solubilization buffer and analyzed by Western blotting for the presence of the CYP2E1 variants. The cytoplasmic-oriented ER protein Dpm1p and the lumenal ER protein KAR2p were included as controls to verify the digestion.

DISCUSSION

From previous studies on mammalian cells we know that a small fraction of CYP2E1 is transported to mitochondria, where it is imported and processed to a shorter, soluble and catalytically active variant (*19, 21*). Initial experiments with yeast as a model system for mitochondrial transport of NH_2-terminally truncated variants of CYP2E1 showed that these truncated enzymes were also found to be associated with the mitochondria in a similar manner as occurred in mouse hepatoma cells. However, instead of being imported and processed, these CYP2E1 variants were found to be associated with the outer membrane of mitochondria. With this in mind, we conducted the current investigation with two main focuses: first, to examine which part of the enzyme is responsible for the mitochondrial localization of these CYP2E1 variants in yeast, and second, to find out specific regions of the enzyme that are responsible for this membrane association.

Examination of the NH_2-terminus of CYP2E1 reveals that there are two putative mitochondrial targeting sequences present, one from amino acids 51 to 64 and a second one from 75 to 94 (underlined sequences in Figure 1A) (*20, 21*). Typically these sequences are found to be rich in positively charged and hydrophobic amino acids with very few or no negatively charged residues at all, and in addition these sequences also have the potential to form an amphiphilic α-helix (*35, 36*). The results from the present study demonstrate that removal of the hydrophobic transmembrane domain of CYP2E1 in yeast also results in a dramatic change in the intracellular localization: while wt2E1 is exclusively found in the microsomal fraction, Δ29-2E1 is only seen in the mitochondrial fraction (Figures 3 and 4). As shown in the mammalian system, also in yeast the deletion of the first putative mitochondrial targeting signal, as in Δ64-2E1, did not significantly affect its intracellular localization: the majority of Δ64-2E1 protein was still found to be associated with the mitochondrial fraction, although a small but significant amount was found in the vacuolar fractions. Only when the second putative mitochondrial targeting signal was entirely deleted (Δ95-2E1) or modified (Δ82mut-2E1) was this mitochondrial association completely lost. Partial deletion (Δ82-2E1) of this region resulted in a more broad distribution, with recovery of the protein in mainly the mitochondrial and vacuolar fractions. The results from the present study in part agree with those from the mammalian studies. In yeast, deletion of the hydrophobic transmembrane domain of CYP2E1 also results in mitochondrial localization of the truncated protein, which was lost when the region between amino acids 75 and 94 (containing the second putative mitochondrial targeting signal) was either modified or deleted. There are, however, differences between yeast and hepatoma cells regarding the targeting of CYP2E1 as exemplified by the truncated versions Δ82-2E1 and Δ95-2E1, which lose their mitochondrial targeting in the mammalian system and display a cytoplasmic staining pattern when examined by immunofluorescence microscopy (*21*), whereas in yeast Δ82-2E1 is found to be associated with the mitochondrial, vacuolar, and to a lesser extent the microsomal fractions and Δ95-2E1 is found almost exclusively with the vacuolar fraction. These results indicate that the mitochondrial import machinery as well as the mitochondrial targeting sequences in yeast and mammalian cells are not completely exchangeable. Interestingly, in a previous study with yeast as a recombinant system for CYP11A1 expression, the presequence of CYP11A1 was replaced by

Table 2: Catalytic Activity of the CYP2E1 Variants[a]

plasmid	NADPH supported [pmol of 6-hydroxy-chlorzoxazone (mg of protein)$^{-1}$ min^{-1}]	CuOOH supported [pmol of 6-hydroxy-chlorzoxazone (mg of protein)$^{-1}$ min^{-1}]
	Microsomes	
V60	3.0 ± 1.0	0.4 ± 0.2
wt2E1	610 ± 21[b]	10.6 ± 1.0[b]
Δ82mut-2E1	<3	1.6 ± 1.2[b]
Δ95-2E1	<3	1.6 ± 0.3[b]
	Mitochondria	
V60	4.9 ± 2.4	
Δ29-2E1	36.9 ± 1.3[b]	
Δ64-2E1	20.5 ± 1.8[b]	
Δ82-2E1	9.1 ± 0.2	

[a] The subcellular fractions, microsomes for wt2E1, Δ82mut-2E1, and Δ95-2E1 and mitochondria for Δ29-2E1, Δ64-2E1 and Δ82-2E1, were monitored for either NADPH- or cumene hydroperoxide- (CuOOH-) supported formation of 6-hydroxychlorzoxazone. The incubation time was 30 min, and 100 μg of total protein was used per incubation. Data are represented as mean ± SEM of at least three independent experiments. [b] Statistically significant difference compared to the V60 control ($P < 0.05$).

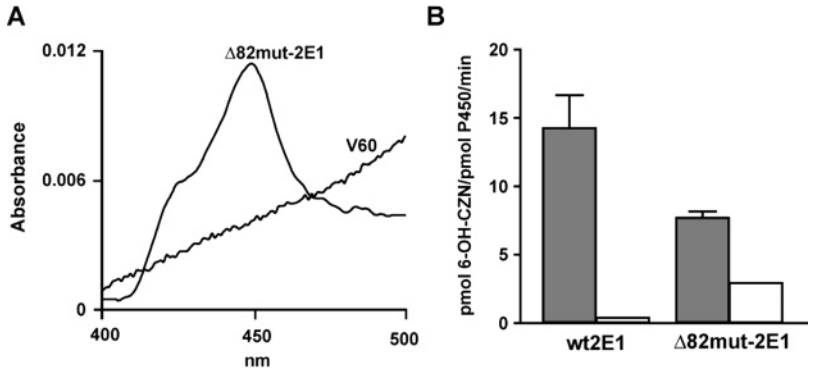

FIGURE 7: Reduced CO spectrum and catalytic activity of Δ82mut-2E1. (A) Reduced carbon monoxide spectra of the 100000*g* supernatant after treatment of the microsomal fraction isolated from yeast expressing Δ82mut-2E1 with 0.5 M potassium phosphate. Supernatant obtained from V60-transformed yeast treated in the same way was included as a control. (B) Formation of 6-hydroxychlorzoxazone (6-OH-CZN) was determined in the microsomal pellet for wt2E1 and 100000*g* supernatant after phosphate treatment for Δ82mut-2E1 (shaded bars). Assays were performed in the presence of 100 μM cumene hydroperoxide as an electron donor, and incubation time was 2.5 min. Data are shown as mean ± SEM of at least three independent experiments. The background activities determined in the same amount of microsomes (for wt2E1) and the supernatant after phosphate treatment (for Δ82mut-2E1) isolated from V60-transfected cells are shown as open bars. Note that the expression of wt2E1 was carried out at 28 °C and that the expression of Δ82mut-2E1 was done at room temperature.

that of yeast cytochrome *c* oxidase subunit VI (COX VI) in order to obtain more efficient mitochondrial targeting and import followed by proteolytic processing in the matrix to the mature catalytic active form (*37*). In addition, the mitochondrial expression levels of bovine heart mitochondrial ADP/ATP carrier in the yeast mitochondrial membrane were greatly improved when its NH_2-terminal region was replaced by the NH_2-terminus of the yeast form of this protein (*38*).

Another difference observed was for the N^{2+}2E1 variant, where introduction of two positively charged amino acids in the hydrophobic NH_2-terminal transmembrane domain of CYP2E1 did not result in mitochondrial targeting and processing to Δ2E1, as was previously observed in the mammalian system. It was suggested that the introduction of these mutations could possibly compromise the binding of the SRP and subsequent cotranslational insertion in the ER membrane. This would result in the translation of the entire protein on cytosolic ribosomes, resulting in the exposure of the mitochondrial targeting signal, after which N^{2+}2E1 would be imported and processed by the mitochondria (*21*). Also in yeast, cotranslational protein targeting to the ER in a SRP-dependent manner is an important pathway for both secretory and membrane-bound proteins. However, when the SRP or the SRP receptor was depleted in *S. cerevisiae*, protein targeting to the ER, although less efficient, still occurred in a SRP-independent manner (*39*−*41*). This indicates that yeast can target proteins that are normally cotranslationally targeted in a SRP-dependent manner in a SRP-independent manner, either in a cotranslational or most likely a posttranslational fashion to the ER membrane. We hypothesize, therefore, that in yeast the N^{2+}2E1 variant, in which the SRP binding site has been altered, is still efficiently targeted posttranslationally to the ER membrane independently of the SRP.

Our findings from this report and the previous studies (*20*, *21*) are in sharp contrast to a recent study that identified a region of amino acids 21−31 responsible for mitochondrial targeting of CYP2E1 by both cellular and in vitro approaches (*42*). In cDNA-transfected COS cells, the mitochondrial targeting was abolished after deletion of the first 36 amino acids. At present it is not clear why this discrepancy between this study and our previous investigations occurs. In our hands, no detectable wt2E1 was transported to mitochondria in cDNA-transfected yeast (this study) or mouse hepatoma cells (*20*, *19*, *21*). Mitochondrial import was only seen after alteration or removal of the SRP binding sequence, located at the most NH_2-terminal part of the enzyme, rendering transcripts that can be translated by cytosolic ribosomes and thereby escape ER targeting. A possible explanation for the difference between these studies might be the different cellular systems used. Attempts in our laboratory were made to express the N^{2+}2E1 as well as the Δ29-2E1 variant in COS-1 cells. However, these experiments revealed that in the case of Δ29-2E1 no protein could be detected despite the presence of mRNA, whereas N^{2+}2E1 was solely found to be present in the full-length ER form, suggesting that mitochondrial targeting and processing does not occur in the COS-1 cells (E. Neve, unpublished observations).

All the variants tested were completely digested with the highest concentration of proteinase K even in the absence of detergent, conditions under which proteins facing the cytosolic side of the membranes are digested. This shows that wt2E1 assumes the expected topology in the ER membrane with the catalytic site facing the cytosol or type I orientation. Also, N^{2+}2E1 was solely present in this type I orientation, unlike in the hepatoma cells, where a small fraction of N^{2+}2E1 was present in a type II orientation where the catalytic site was facing the lumen of the ER (*19*). The digitonin digestion demonstrated that Δ29-2E1 displayed the same behavior as the mitochondrial outer membrane protein porin, suggesting that Δ29-2E1 was indeed associated with the mitochondrial outer membrane. However, at present we cannot exclude that a small fraction was imported into the mitochondria as indicated by the small amount of Δ29-2E1 that was resistant toward digestion at the lowest concentration of proteinase K.

Δ29-2E1 and Δ64-2E1 were found to be tightly associated with the mitochondrial membrane despite the removal of the region that has been identified as the membrane anchor for P450s (*4*, *3*). Not until the first 82 amino acids were deleted was a significant effect observed, with about equal amounts being found in the soluble and membrane fraction after bicarbonate treatment. Further truncation (Δ95-2E1) as well as the mutation of two hydrophobic residues in Δ82-2E1

(Δ82mut-2E1) resulted in the near-complete recovery of these proteins in the soluble fraction after bicarbonate treatment. This indicates that other regions of the protein are able to form a tight interaction with the lipid bilayer. When expressed in *Escherichia coli,* CYP2E1 lacking the hydrophobic transmembrane domain was shown to be strongly associated with the bacterial inner cell membrane (*43*, *44*). The region between helices F and G, the F−G loop, has been suggested to be able to interact with the membrane (*45*). Mutation of six amino acids in this region in addition to removal of the NH_2-terminal membrane anchor of CYP2C5 resulted in a monomeric and soluble enzyme (*46*). It is noteworthy that CYP2E1 has constitutively four out of these six mutated amino acids in the F−G loop of CYP2C5, suggesting that other regions could be of importance for membrane interactions of CYP2E1. Hence our efforts to determine the membrane-binding properties of CYP2E1 were concentrated on the NH_2-terminal portion of this enzyme with focus on the B-helix. Deletion of the region between amino acids 82 and 95 in CYP2E1 resulted in a protein that was loosely associated with the membrane of the vacuole; the majority could be released by treatment with bicarbonate or a high concentration of potassium phosphate. The results obtained in those experiments indicate that except for Δ82-2E1 and Δ95-2E1, the other CYP2E1 variants, wt2E1, N^{2+}-2E1, Δ29-2E1, and Δ64-2E1, are integral membrane proteins or, more likely in the case of the truncated variants, strongly associated with the membrane surface of the ER or mitochondria. On the contrary, Δ82mut-2E1 as well as Δ95-2E1 was easily solubilized when treated with bicarbonate or phosphate, suggesting that these proteins were peripherally associated with the vacuolar membrane. Δ82-2E1 was only effectively solubilized at the highest phosphate concentration, indicating a much stronger membrane interaction. These results imply that the region between amino acids 82 and 95, the B helix, is involved in membrane binding and that this binding is mainly mediated by electrostatic interactions. In the sucrose gradient both Δ64-2E1 and Δ82-2E1 were found to be present not only in the mitochondrial fraction but small amounts also were recovered in the upper part of the gradient. One interpretation of this observation is that these two variants detach from the mitochondrial membranes as they sediment through the gradient, as was previously suggested for the soluble rabbit CYP2C5 variants (*34*).

All CYP2E1 variants used in this study except for Δ95-2E1 and Δ82mut-2E1 were shown to display catalytic activity in the presence of NADPH (Table 2). The yeast strain used in this study has been engineered to overexpress the yeast NADPH cytochrome P450 reductase that is able to transfer electrons to the recombinant expressed P450s (*26*). Previously we have shown that in hepatoma cells the mitochondrially located and soluble Δ2E1 lacking about 100 amino acids was dependent on adrenoredoxin and adrenoredoxin reductase for its catalytic activity (*21*). Reconstitution of Δ29-2E1, Δ64-2E1, and Δ82-2E1 with adrenodoxin and adrenodoxin reductase did not result in any enhanced catalytic activity, suggesting that these mitochondrial electron transfer proteins are not able to efficiently couple with these CYP2E1 variants. The Δ82mut-2E1 and Δ95-2E1 variants did not productively interact with either the yeast P450 reductase or the adrenodoxin−adrenodoxin reductase system but converted the CYP2E1 substrate chlorzoxazone efficiently in cumene hydroperoxide-supported reactions. Moreover, after phosphate treatment resulting in the solubilization of Δ82mut2E1, a reduced CO spectrum could be recorded, indicating the proper incorporation of the heme hence supporting the observed catalytic activity. The specific activity of this soluble 2E1 variant was found to be about 35% when compared with wt2E1. The finding that an extensive NH_2-terminal deletion still results in a catalytically active protein is surprising and indicates that the catalytic site is able to properly fold in the absence of the first 82 amino acids. Interestingly, deletion of the first 102 NH_2-terminal amino acids of human CYP19 (aromatase) resulted in a protein that was catalytically active when expressed in CHO cells (*47*).

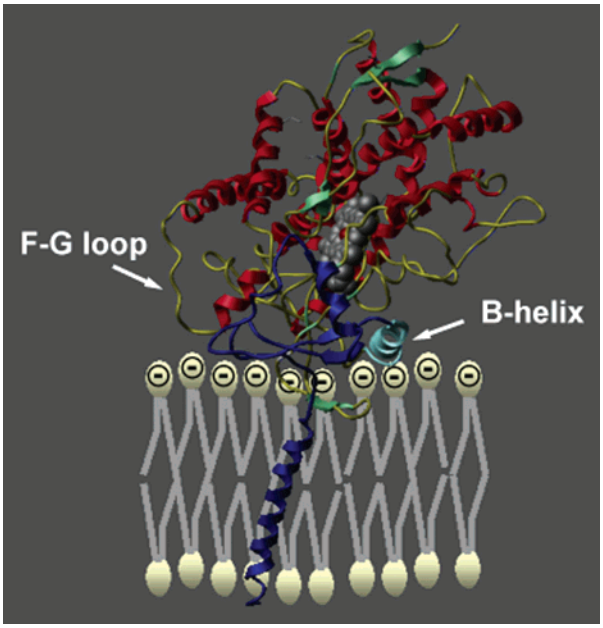

FIGURE 8: Homology model of rat CYP2E1 based on the crystal structure of CYP2C5. The picture depicts a possible orientation of the protein partly embedded in the phospholipid bilayer. The overall positive charge of the B-helix interacts with the net negative charge of the membrane (indicated by minus signs). The NH_2-terminal segment, shown in blue, corresponds to amino acids 1−95. Arrows indicate the F−G loop and the B-helix. The light blue part, which includes the B-helix, indicates regions important for targeting and membrane binding as revealed from the present study. Helixes are colored red, sheets are light green, and the heme in the center of the protein is depicted in gray.

Our data indicate that a soluble product of CYP2E1 is obtained only when the B-helix is removed as in Δ95-2E1 or when two negative amino acids replacing hydrophobic leucines are introduced into the amphipatic B-helix as in Δ82mut-2E1. Analysis of the helix-charge distribution reveals that the two mutations substituting the leucines at positions 90 and 91 with the negatively charged aspartic acid abolish the amphipathic structure of this side of the B-helix and introduce a negative charge between the two positive lysines (Figure 1B). Our interpretation is that one side of the B-helix has a net positive charge and is facing the membrane, which has a strong net negative charge. The introduction of aspartate in positions 90 and 91 changes the overall charge of the B-helix so that the enzyme is repelled from the negative membrane as visualized in Figure 1B. The Δ82mut-2E1 and Δ95-2E1 variants are thus very easily detached from membranes, making them interesting objects

for future crystallization attempts. Several of the enzymes in the CYP2 family have a B-helix sequence very similar to that of CYP2E1, which may suggest that these enzymes interact with membranes in a similar manner as CYP2E1.

A CYP2E1 model was generated in an automated protein-modeling program using the mammalian CYP2C5 crystal structure coordinates (Figure 8). The resulting model was also extended with an additional 30 amino acids, which was artificially put on the structure to simulate the NH_2-terminal hydrophobic membrane-spanning part. The model clearly depicts how the positively charged face of the B-helix might interact with the negative net charge of the lipid bilayer.

It is concluded that yeast can be used as a model system for the intracellular targeting of rat CYP2E1 and NH_2-terminal deletion mutants thereof and other mammalian proteins as well, although differences with respect to mitochondrial import and processing may exist. CYP2E1 lacking the hydrophobic NH_2-terminal transmembrane domain is specifically targeted to the mitochondria but, unlike in the mammalian cells, not efficiently imported and further processed to a soluble from. The region between amino acids 82 and 95, the so-called B-helix, was shown to be responsible for the mitochondrial association of these NH_2-terminally truncated CYP2E1 forms. Moreover, this region was also shown to be required for the interaction of these truncated proteins with the membranes, and a change in the net charge of the B-helix resulted in a soluble catalytically active form of the enzyme that might be a relevant target for future crystallization studies.

ACKNOWLEDGMENT

We thank the group of Per Ljungdahl, Ludwig Institute for Cancer Research, Karolinska Institutet, for useful discussions and their generous gift of the KAR2p antibodies and Professor Rita Bernhardt, University of Saarbrücken, Germany, for her generous gift of adrenodoxin and adrenodoxin reductase.

REFERENCES

1. Bar-Nun, S., Kreibich, G., Adesnik, M., Alterman, L., Negishi, M., and Sabatini, D. D. (1980) *Proc. Natl. Acad. Sci. U.S.A. 77*, 965−969.
2. Monier, S., Van Luc, P., Kreibich, G., Sabatini, D. D., and Adesnik, M. (1988) *J. Cell. Biol. 107*, 457−470.
3. Sakaguchi, M., Mihara, K., and Sato, R. (1984) *Proc. Natl. Acad. Sci. U.S.A. 81*, 3361−3364.
4. Ahn, K., Szczesna-Skorupa, E., and Kemper, B. (1993) *J. Biol. Chem. 268*, 18726−18733.
5. Murakami, K., Mihara, K., and Omura, T. (1994) *J. Biochem. (Tokyo) 116*, 164−175.
6. Szczesna-Skorupa, E., Chen, C. D., and Kemper, B. (2000) *Arch. Biochem. Biophys. 374*, 128−136.
7. Bondoc, F. Y., Bao, Z., Hu, W. Y., Gonzalez, F. J., Wang, Y., Yang, C. S., and Hong, J. Y. (1999) *Biochem. Pharmacol. 58*, 461−463.
8. Ronis, M. J. J., Lindros, K. O., and Ingelman-Sundberg, M. (1996) in *Cytochromes P450, Pharmacological and Toxicological Aspects* (Ioannides, C., Ed.) CRC Press, Inc., Boca Raton, FL, pp 211−239.
9. Sohn, O. S., Fiala, E. S., Requeijo, S. P., Weisburger, J. H., and Gonzalez, F. J. (2001) *Cancer Res. 61*, 8435−8440.
10. Sumner, S. C., Fennell, T. R., Moore, T. A., Chanas, B., Gonzalez, F., and Ghanayem, B. I. (1999) *Chem. Res. Toxicol. 12*, 1110−1116.
11. Zaher, H., Buters, J. T., Ward, J. M., Bruno, M. K., Lucas, A. M., Stern, S. T., Cohen, S. D., and Gonzalez, F. J. (1998) *Toxicol. Appl. Pharmacol. 152*, 193−199.
12. Ekstrom, G., and Ingelman-Sundberg, M. (1989) *Biochem. Pharmacol. 38*, 1313−1319.
13. Chen, Q., and Cederbaum, A. I. (1998) *Mol. Pharmacol. 53*, 638−648.
14. Nieto, N., Friedman, S. L. and Cederbaum, A. I. (2002) *Hepatology 22*, 62−73.
15. Ronis, M. J., Johansson, I., Hultenby, K., Lagercrantz, J., Glaumann, H., and Ingelman-Sundberg, M. (1991) *Eur. J. Biochem. 198*, 383−389.
16. Neve, E. P., Eliasson, E., Pronzato, M. A., Albano, E., Marinari, U., and Ingelman-Sundberg, M. (1996) *Arch. Biochem. Biophys. 333*, 459−465.
17. Pahan, K., Smith, B. T., Singh, A. K., and Singh, I. (1997) *Free Radic. Biol. Med. 23*, 963−971.
18. Eliasson, E., and Kenna, J. G. (1996) *Mol. Pharmacol. 50*, 573−582.
19. Neve, E. P., and Ingelman-Sundberg, M. (2000) *J. Biol. Chem. 275*, 17130−17135.
20. Neve, E. P., and Ingelman-Sundberg, M. (1999) *FEBS Lett. 460*, 309−314.
21. Neve, E. P., and Ingelman-Sundberg, M. (2001) *J. Biol. Chem. 276*, 11317−11322.
22. Fiedler, B., and Scheiner-Bobis, G. (1996) *J. Biol. Chem. 271*, 29312−29320.
23. Kuroda, S., Itoh, Y., Miyazaki, T., Otaka-Imai, S., and Fujisawa, Y. (1989) *Gene 78*, 297−308.
24. Bylund, J., Hidestrand, M., Ingelman-Sundberg, M., and Oliw, E. H. (2000) *J. Biol. Chem. 275*, 21844−21849.
25. Guengerich, F. P., Brian, W. R., Sari, M. A., and Ross, J. T. (1991) *Methods Enzymol. 206*, 130−145.
26. Pompon, D., Louerat, B., Bronine, A., and Urban, P. (1996) *Methods Enzymol. 272*, 51−64.
27. Loeper, J., Le Berre, A., and Pompon, D. (1998) *Mol. Pharmacol. 53*, 408−414.
28. Lithgow, T. (2000) *FEBS Lett. 476*, 22−26.
29. Neupert, W. (1997) *Annu. Rev. Biochem. 66*, 863−917.
30. Komiya, T., Rospert, S., Schatz, G., and Mihara, K. (1997) *EMBO J. 16*, 4267−4275.
31. Egner, R., Mahe, Y., Pandjaitan, R., and Kuchler, K. (1995) *Mol. Cell. Biol. 15*, 5879−5887.
32. Fujiki, Y., Hubbard, A. L., Fowler, S., and Lazarow, P. B. (1982) *J. Cell. Biol. 93*, 97−102.
33. Hartl, F. U., Schmidt, B., Wachter, E., Weiss, H., and Neupert, W. (1986) *Cell 47*, 939−951.
34. Williams, P. A., Cosme, J., Sridhar, V., Johnson, E. F., and McRee, D. E. (2000) *Mol. Cell 5*, 121−131.
35. Roise, D., and Schatz, G. (1988) *J. Biol. Chem. 263*, 4509−4511.
36. von Heijne, G. (1986) *EMBO J. 5* (6), 1335−1342.
37. Dumas, B., Cauet, G., Lacour, T., Degryse, E., Laruelle, L., Ledoux, C., Spagnoli, R., and Achstetter, T. (1996) *Eur. J. Biochem. 238*, 495−504.
38. Hatanaka, T., Takemoto, Y., Hashimoto, M., Majima, E., Shinohara, Y., and Terada, H. (2001) *Biol. Pharm. Bull. 24*, 595−599.
39. Hann, B. C., and Walter, P. (1991) *Cell 67*, 131−144.
40. Ng, D. T., Brown, J. D., and Walter, P. (1996) *J. Cell Biol. 134*, 269−278.
41. Ogg, S. C., Poritz, M. A., and Walter, P. (1992) *Mol. Biol. Cell 3*, 895−911.
42. Robin, M. A., Anandatheerthavarada, H. K., Biswas, G., Sepuri, N. B., Gordon, D. M., Pain, D., and Avadhani, N. G. (2002) *J. Biol. Chem. 277*, 40583−40593.
43. Larson, J. R., Coon, M. J., and Porter, T. D. (1991) *J. Biol. Chem. 266*, 7321−7324.
44. Pernecky, S. J., Larson, J. R., Philpot, R. M., and Coon, M. J. (1993) *Proc. Natl. Acad. Sci. U.S.A. 90*, 2651−2655.
45. Graham-Lorence, S. E., and Peterson, J. A. (1995) in *Advances in Molecular and Cell Biology, Vol. 14. Physiological Functions of Cytochrome P450 in Relation to Structure and Regulation* (Jefcote, C., Ed.), JAI Press Inc., Greenwich, CT, pp 57−79.
46. Cosme, J., and Johnson, E. F. (2000) *J. Biol. Chem. 275*, 2545−2553.
47. Kao, Y. C., Higashiyama, T., Yarborough, C., Osawa, Y., and Chen, S. (1999) *Steroids 64*, 422−429.

BI035193S